

Effect of genetic modification of tyrosine-185 on the proton pump and the blue-to-purple transition in bacteriorhodopsin

(bacteriorhodopsin photocycle/site-specific mutants/tyrosine deprotonation/pH dependence/protein conformation changes)

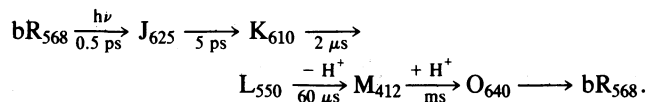
DU-JEON JANG*[†], M. A. EL-SAYED*[‡], LAWRENCE J. STERN[§]||, TATSUSHI MOGI[§]||, AND H. GOBIND KHORANA[§]

*Department of Chemistry and Biochemistry, University of California, Los Angeles, CA 90024; and [†]Departments of Chemistry and Biology, Massachusetts Institute of Technology, Cambridge, MA 02139

Contributed by M. A. El-Sayed, December 19, 1989

ABSTRACT The retinylidene chromophore mutant (Y185F) of bacteriorhodopsin, in which Tyr-185 is substituted by phenylalanine, is examined and compared with wild-type bacteriorhodopsin expressed in *Escherichia coli*; both were reinstated similarly in vesicles. The Y185F mutant shows (at least) two distinct spectra at neutral pH. Upon light absorption, the blue species (which absorbs in the red) behaves as if “dead”—i.e., neither its tyrosine nor its protonated Schiff base undergoes deprotonation nor does its tryptophan fluorescence undergo quenching. This result is unlike either the purple species (which absorbs in the blue) or wild-type bacteriorhodopsin expressed in *E. coli*. As the pH increases, both the color changes and the protonated Schiff base deprotonation efficiency suggest a blue-to-purple transition of the Y185F mutant near pH 9. If this blue-to-purple transition of Y185F corresponds to the blue-to-purple transition of purple-membrane (native) bacteriorhodopsin (occurring at pH 2.6) and of wild-type bacteriorhodopsin expressed in *E. coli* (occurring at pH 5), the protein-conformation changes of this transition as well as the protonated Schiff base deprotonation may be controlled not by surface pH alone, but rather by the coupling between surface potential and the general protein internal structure around the active site. The results also suggest that Tyr-185 does not deprotonate during the photocycle in purple-membrane bacteriorhodopsin.

The retinylidene protein bacteriorhodopsin (bR), the other photosynthetic system besides chlorophyll pigments, is a protein pigment found in the purple membrane of *Halobacterium halobium* (1, 2). Light-adapted bR contains an all-*trans*-retinal, which is covalently bound via a protonated Schiff base (PSB) linkage to the apoprotein, known as bacterioopsin (bO) (1, 3, 4). Upon absorption of visible light, bR at neutral pH undergoes a photochemical cycle (5, 6):



As a result, bR translocates protons from inside to outside the cell, increasing the proton concentration on the outer surface of the membrane (7). The created proton gradient across the membrane is then used to transform ADP into ATP in the final step of *H. halobium* photosynthesis (2, 5, 8).

Elucidation of the mechanism of this light-driven proton pump is of fundamental interest from chemical and biological points of view. In an approach to understanding the mechanism, a variety of site-directed mutagenetic methods now permit alteration of any amino acid residue in bO (9–12). Thus, bO mutants that contain single-amino acid substitutions have been prepared and studied by a number of bio-

chemical and biophysical techniques to test current hypotheses regarding bR structure and function (13–22).

Previously, the proton pumping across the membrane has been postulated to occur as protons are transferred through amino acid side chains (23, 24). Among the several models involving specific residues (25), a role for tyrosine in light-driven proton pumping by bR was suggested. Tyrosine deprotonates on the same time scale as M₄₁₂ formation (26–29). bR was found to contain 11 tyrosine residues of 248 amino acid residues in its polypeptide chain (30). The retinal absorption maximum and the proton-pumping efficiency were measured for each of the 11 possible bR mutants containing a single Tyr → Phe substitution (17). Among the 11 mutants studied, the Tyr-185 → Phe bR expressed in *Escherichia coli* (Y185F mutant) has the lowest absorption energy (λ_{max} = 573 nm), the smallest steady-state proton-pumping level (52%) compared with wild-type bR expressed in *E. coli* (ebR), and the slowest initial proton-pumping rate (36% compared with ebR) (17).

The low-temperature UV-visible difference spectra showed (22) that the Y185F mutant has a red-shifted photo-product (λ_{max} = 665 nm) in addition to the normal K intermediate (λ_{max} = 622 nm), indicating that the Y185F mutant contains more than one photochemically active species (22). From Fourier transform infrared spectroscopy (FTIR) difference spectra, Braiman *et al.* (13) concluded that Tyr-185 gains a proton during the bR₅₆₈ → K₆₁₀ photoreaction and loses it when the M₄₁₂ intermediate is formed, as had been concluded earlier (31). They proposed that Tyr-185 is ionized and serves as a counterion to the PSB in purple-membrane bR₅₆₈. This fact emphasizes the importance of Tyr-185 to the photocycle. If Tyr-185 is, indeed, a counterion, its replacement with neutral phenylalanine should greatly change the kinetics of the photocycle (or stop it). Furthermore, if Tyr-185 deionizes during M₄₁₂ formation (13), the Y185F mutant should not show the transient absorption at 296 nm assigned to tyrosinate ion (Tyr⁻) (26, 27).

Replacing bound metal cations by hydrogen ions changes the purple into blue bR (1, 33–36). This finding was explained by protonating the counterion at low pH (34, 37); the observed changes in protein conformation accompanying this transition (35), as well as the need for more than one surface metal cation to regenerate the purple form (38), indicated the importance of

Abbreviations: bO, bacterioopsin; bR, bacteriorhodopsin; pmbR, purple-membrane bR; ebR, wild-type bR expressed in *Escherichia coli*; PSB, protonated Schiff base; Tyr⁻, tyrosinate ion; Y185F, Tyr-185 → Phe bR expressed in *E. coli*.

[†]Present address: Spectroscopy Laboratory, Korea Standards Research Institute, Daedeok Science Town, Taejeon 305-606, Republic of Korea.

[‡]To whom reprint requests should be addressed.

[§]Present address: Department of Biochemistry and Molecular Biology, Harvard University, Cambridge, MA 02138.

||Present address: Department of Biology, Faculty of Science, University of Tokyo, Hongo, Bunkyo-ku, Tokyo 113, Japan.

The publication costs of this article were defrayed in part by page charge payment. This article must therefore be hereby marked “advertisement” in accordance with 18 U.S.C. §1734 solely to indicate this fact.

surface charges in controlling the protein-conformation changes required for this transition. The importance of surface charges (38–40), in general, and surface pH (41–43), in particular, has been concluded from studies modifying the surface by decreasing the pH, removing surface-bound metal cations (38) or the negatively charged lipids (41–43). The importance of the interaction between surface charges and internal protein charges and dipoles had been suggested (38, 40), but direct experimental tests were lacking. In the present work, the pH at which the purple-to-blue transition takes place was studied in ebR and its Y185F mutant. Both have the same lipid (surface) structure but have quite different active-site structures [recently shown by retinal CD spectroscopy (44)]. The results strongly support the importance of the structure of the active site in determining the transition pH, which was quite different for ebR and the Y185F mutant.

MATERIALS AND METHODS

Construction of the gene coding for the Y185F mutant and preparation of mutant bO apoproteins by using a heterologous (*E. coli*) expression system have been described (16, 45, 46). Purified bO was regenerated with retinal and reconstituted in vesicles in 1:1 weight ratio with polar lipids from *H. halobium* (45, 46) by using the procedures of Popot *et al.* (47). The fraction of mutant apoprotein that bound a chromophore was $\approx 50\%$.

Steady-state absorption spectra were measured with a Hewlett-Packard 8451 diode-array spectrometer or a Cary 219 UV/visible spectrometer. For measuring the transient absorption of M_{412} and Tyr^- formation, photolysis was accomplished with pulses from a N_2 -pumped dye laser (LN1000 and LN102, Photochemical Research Associates, Oak Ridge, TN) run at a repetition rate of 1–5 Hz. Different laser dyes were used to study wavelength dependence of the photolysis. The photolyzing laser pulse had an energy of $\approx 50 \mu J$ with a pulse width of ≈ 0.5 ns and was collimated to ≈ 3 -mm spot size. The probing light from a 100-W Hg arc lamp (401, Pek Labs, Sunnyvale, CA) was passed through the sample and focused into a 0.25-m spectrometer (82-410, Jarrell-Ash, Waltham, MA). The wavelength-selected probe light was detected by a photomultiplier tube (RCA1P28A, Lancaster, PA) and recorded with a transient digitizer (Biomation 805 waveform recorder, Santa Clara, CA) interfaced to a microcomputer (Apple II+, Cupertino, CA). Signals were averaged for 1×10^3 laser shots and then converted to transient absorption in OD.

For kinetic measurements of tryptophan-fluorescence quenching during the bR photocycle, the steady-state excitation wavelength of tryptophan was selected from the Hg lamp by using a narrow-band interference filter (280 ± 5 nm). Tryptophan fluorescence in the 320- to 400-nm range was selected with a combination of filters, including $CuSO_4$ solution in water. The tryptophan-fluorescence intensity change after photolysis by the laser pulse was monitored by a photomultiplier tube (EMI 9813GB, England) and recorded with the transient digitizer.

RESULTS

Absorption and Light-Dark Adaptation. The absorption spectrum of the light-adapted Y185F mutant (λ_{max} , ≈ 570 nm) at neutral pH is largely shifted toward the red and is broader compared with that of ebR, as reported (17, 20). Fig. 1 shows that the dark-adapted form has a broad spectrum with two clearly resolved maxima. The light-to-dark adaptation takes place in ≈ 1 min for both ebR and the Y185F mutant, which is shorter than that reported for bR in purple-membrane bR (pmbR) (47). For the Y185F mutant sample at pH 6, the absorption change at 540 nm by dark-to-light adaptation is

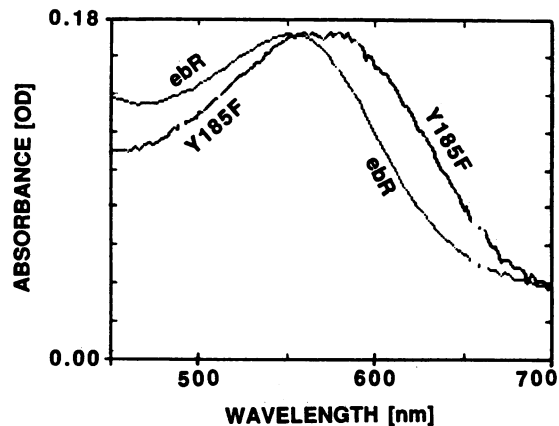


FIG. 1. Absorption spectra of dark-adapted ebR and the Y185F mutant. The Y185F spectrum shows two absorption maxima at ≈ 562 and ≈ 584 nm, whereas that of ebR shows one absorption maximum at 552 nm.

$\approx 40\%$ of that of ebR at the same concentration. This fact indicates that a smaller fraction of bR molecules in Y185F samples undergoes the cis-to-trans isomerization during dark-to-light adaptation, as compared with ebR.

In dark adaptation of the Y185F mutant, the absorption maximum of the molecules that undergo isomerization shifts to the blue, resulting in the appearance of two absorption maxima at 562 nm and 584 nm (Fig. 1). This observation, thus, suggests the presence of (at least) two different species in the Y185F samples: one species undergoes the cis-trans isomerization (and can thus undergo the proton-pumping cycle), but the other does not. This fact might also explain the lower proton-pumping efficiency in the Y185F mutant as compared with ebR (17).

Deprotonation Probability and Kinetics of the PSB. Fig. 2 shows that the M_{412} formation efficiency of the Y185F mutant relative to that in ebR supports the above conclusion. These results suggest that at least two species are present in the Y185F mutant. The species absorbing at longer wavelength may not pump protons or may pump with much reduced efficiency.

The Y185F mutant has two formation components of M_{412} , as seen in ebR and pmbR (29). The fast component has a larger amplitude in the Y185F mutant than in ebR, which is larger than in pmbR at pH 6. As pH increases, the relative amplitude of the fast component increases, but the rates of the two components do not change as much for ebR as for pmbR (29).

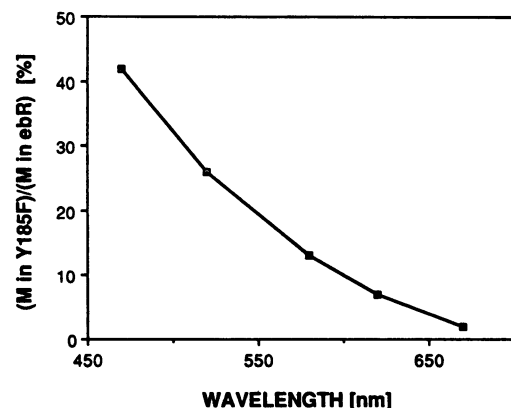


FIG. 2. Photolysis wavelength dependence of relative M_{412} (M) formation efficiency of the Y185F mutant (relative to that of ebR) at pH 6. M_{412} formation efficiency was calculated from the absorbance change at 405 ± 5 nm.

If heterogeneity causes the different components of M_{412} , either the difference in lipid composition or the protein-conformation changes could lead to the observed variation. The numbers given in Table 1 for the formation rates of M_{412} in ebR are faster by a factor of ≈ 4 than in native bR. Because the rate of protein-conformation changes is believed to determine the rate of M_{412} formation (29), this result suggests that since the lipid differs in both bR types, lipid composition and its surface charges might control the rate of protein-conformation changes during deprotonation.

pH Dependence of the Absorption and M_{412} Formation Efficiency. Fig. 3 shows the pH dependency of the bound retinal absorption maximum wavelengths and M_{412} formation efficiencies for the Y185F mutant and ebR. Both Y185F and ebR bleach at pH <4, and the free retinal remains in solution. The absorption maximum wavelengths of bound retinal for both the Y185F mutant and ebR decrease with increasing pH. However, the Y185F mutant shows a color transition near pH 9, where the ebR wavelength hardly changes with pH. The M_{412} formation efficiency of ebR increases sharply with pH at ≈ 5.5 and levels off above 8. The M_{412} formation efficiency of the Y185F mutant increases most sharply at pH ≈ 9 and levels off above pH 10. The M_{412} formation efficiency per OD unit of the parent absorption at the photolyzing wavelength becomes similar above pH 10 for both ebR and the Y185F mutant, suggesting the presence of only the active bR type in Y185F, as in ebR.

These results suggest that the inactive type of bR in the Y185F mutant becomes active near pH 9, which is similar to the blue-to-purple transition found in pmbR at pH 2.6 (1, 33–36, 48). The sharp increase in M_{412} formation in ebR near pH 5.5 suggests that its blue-to-purple transition occurs at this pH.

Transient Absorption at 296 nm and Its Kinetics. Transient absorption kinetics at ≈ 296 nm during the photocycle at neutral pH show two rise components on the μ s-time scale for pmbR. The fast rise has been ascribed to chromophore isomerization, whereas the slower rise has been ascribed to tyrosine deprotonation (26, 27).

The rise kinetics of transient absorption at 295 ± 5 nm for ebR and the Y185F mutant at pH 6 and 10 are shown in Fig. 4. The kinetics of ebR at pH 6 shows the fast- and slow-rise components, whereas that at pH 10 shows no or very small transient absorption signal at this wavelength. For pmbR, the amplitude of the slow component becomes small or negligible above the pK_a of tyrosine, but the amplitude of the fast component does not change significantly with pH (29). It was shown earlier that the absorption maximum of ebR and the Y185F mutant shifts to shorter wavelength as the sample pH increases. The negligible transient absorption of the fast component at pH 10 for ebR might then suggest that the absorption cross-section of retinal at this wavelength is similar for ebR and its M_{412} intermediate at pH 10. For the Y185F mutant, we

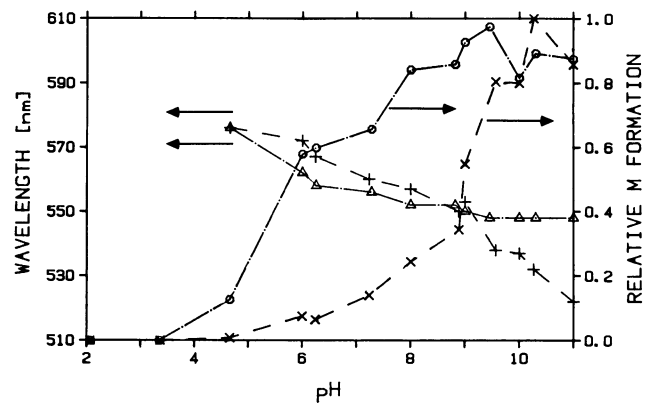


FIG. 3. pH dependence of the bound retinal absorption maximum wavelengths of the Y185F mutant (+) and ebR (Δ) and pH dependence of the M_{412} formation efficiencies of the Y185F mutant (x) and ebR (\circ) [as measured by transient absorption at 405 nm after being normalized by the OD at the photolyzing wavelength (580 nm)]. Arrows refer to vertical axes.

see the slow component only at pH 6 and a negative amplitude of only the fast component at pH 10. The negative change suggests that absorption of the retinal at 295 nm in the Y185F mutant is larger than in its M_{412} intermediate at pH 10.

The deprotonation rates of tyrosine at pH 6 are 1.6×10^4 s $^{-1}$ for ebR, 6.6×10^3 s $^{-1}$ for the Y185F mutant, and 9.2×10^3 s $^{-1}$ (29) for pmbR at pH 6. It is interesting to observe that the ratios of the rates of slow M_{412} formation to that of Tyr $^{-}$ formation are 1.4, ≈ 4 , and ≈ 6 for bR in purple membranes at pH 7 (29), in ebR at pH 6, and in the Y185F mutant at pH 6, respectively. These rates suggest that M_{412} is formed before Tyr $^{-}$ formation during the photocycle and, thus, does not get involved in the proton translocation network in any of these species.

Fig. 4 shows that at pH 6, both ebR and the active component of the Y185F mutant show tyrosine deprotonation. The transient absorption amplitude of tyrosine deprotonation is much smaller for the Y185F mutant than that for ebR. However, when normalized to the absorption for both, Tyr $^{-}$ is formed with the same efficiency as M_{412} in both the Y185F mutant and ebR. If, indeed, the absorption at 296 nm is from Tyr $^{-}$ absorption (26, 27), these results shed doubt (13) on the proposal that Tyr-185 is the tyrosine that deprotonates during M_{412} formation of bR in the active Y185F mutant. These results also question the fact that Tyr-185 is an important counterion (31) used for energy storage of the active component of the Y185F mutant at pH 7. In light of recent NMR results that Tyr $^{-}$ is seen only at very high pH (48) and previous Raman results (49), the absorption at 296 nm could be due to perturbed tryptophan (49). This explanation would be consistent with our observations.

Table 1. pH dependence of the rate constants and relative amplitudes of the two components of M_{412} formation for ebR and the Y185F mutant at room temperature ($\approx 22^\circ\text{C}$)

pH	ebR				Y185F			
	M_{fast}		M_{slow}		M_{fast}		M_{slow}	
	Rate constant*	Relative amplitude †	Rate constant*	Relative amplitude	Rate constant	Relative amplitude	Rate constant	Relative amplitude
6	4	0.32	0.7	0.68	2	0.56	0.4	0.44
8	4	0.48	0.5	0.52	2	0.65	0.2	0.35
9	4	0.62	0.4	0.38	4	0.64	0.3	0.36
10	4	0.67	0.4	0.33	5	0.77	0.3	0.23
6	1.6	0.15	0.18	0.85	Native bR at 25°C^\dagger			
6	0.56	0.37	0.087	0.63	75% delipidated at 25°C^\dagger			

*Rate constant in $k \times 10^5$ sec $^{-1}$.

† See ref. 34.

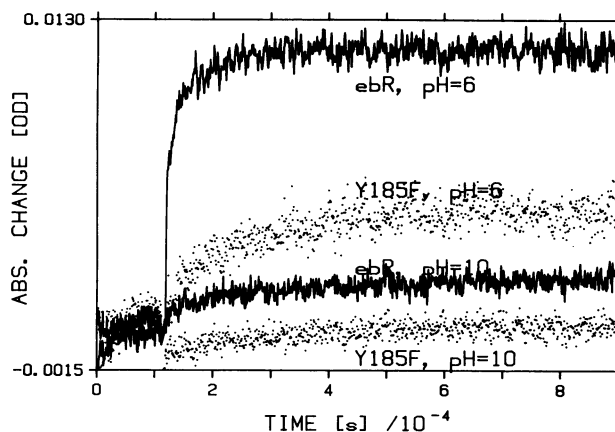


FIG. 4. Formation kinetics of transient absorption (ABS.) at 295 ± 5 nm for ebR and the Y185F mutant at pH 6 and 10. Samples were photolyzed at ≈ 580 nm.

Tryptophan-Fluorescence Quenching During the Cycle. The tryptophan-fluorescence lifetime in bR was shown to have several components attributed to different quenching efficiencies for molecules at different distances (or geometrics) from retinal (40). The probability of quenching changes during the cycle (50–52) and is very sensitive to pH (53) due to changes in protein conformation, attributable to either the cycle (52) or pH (53).

Tryptophan-fluorescence quenching during the cycle is seen for both the Y185F mutant and ebR. The relative quenching efficiency of the Y185F mutant to that of ebR (which is ≤ 1) and its dependence on the photolysis wavelength are similar to those for M_{412} formation. This fact is clarified by the realization that only the active component of the Y185F mutant can go through the photocycle, which changes protein conformation.

DISCUSSION

These results have shown that in the Y185F mutant at least two spectrally distinct species, Y185F₁ and Y185F₂, exist. The species absorbing at relatively shorter wavelength (termed purple Y185F) forms M_{412} intermediate, undergoes transient absorption at 295 nm on the time scale of M_{412} formation, quenches tryptophan fluorescence during the photocycle during M_{412} formation, and exhibits changes in its retinal absorption upon light–dark adaptation. The other species absorbs at relatively longer wavelength (termed blue Y185F) but does not undergo any of these processes. Purple Y185F mutant (species 1) shows very similar kinetics and yield of M_{412} formation to that of ebR. Blue Y185F (species 2) converts to purple Y185F as the pH increases, with an apparent transition pH near 9, which is associated with a distinct color change from purple-blue to purple (see Fig. 3). This behavior is very similar to the conversion of blue bR into purple bR in pmbR. The latter transition is sharper and occurs in acidic pH at 2.6. ebR, which has similar lipid to Y185F, has its apparent blue-to-purple transition occurring at a pH ≈ 5.5 .

The proposal that the transition results from protonating the counterion (34, 37) would require that the counterion changes its pK_a by 3.5. This is possible if the counterion is an aspartate that is hydrogen-bonded to Tyr-185 in ebR (and in pmbR). Replacing by a nonhydrogen bonding agent like phenylalanine could increase its pK_a . By use of Warshel's equation (54),

$$\Delta pK_a = \Delta q \left(\frac{332}{40R} \right) \frac{1}{1.38},$$

where q = charge and R = distance, when retinal is ≈ 20 Å from the surface, the observed ΔpK_a from ebR to Y185F of 3.5 requires a change in interacting charges of 10 units. Thus, the surface charge interacting with the counterion would have to change by 10 units when the pH of the medium shifts from 5.5 to 9.0. Ten units seems too large and suggests that the interaction is not a simple macroscopic one, but rather more complex.

Our results also suggest that the proposal that surface pH induces the transition by simply protonating surface conjugate-acid groups (42, 43) cannot be totally correct; otherwise ebR and the Y-185 mutant would have the same transition pH. Thus, coupling between surface potential (which depends on ionization states of the different surface acidic groups and, thus, the surface pH) and internal charges and dipoles of the amino acids that control the structure of the active site must be critical (38, 40) in determining the transition pH and the protein-conformation changes during blue-to-purple transition. Because change in color correlates faithfully with change in deprotonation of pmbR (53), this coupling must then control the protein-conformation changes leading to deprotonation of the PSB (29, 40, 54).

The conformation change in the purple-to-blue transition shifts retinal absorption to the red and renders the PSB incapable of deprotonation (53). If absorption energy is conceptualized as the energy required to displace the positive charge (the hole) on the PSB to carbon atoms down the chain on the retinal conjugated system, then a lowering of this energy in the blue form might weaken the coupling between the positively charged PSB and its negatively charged counterion(s). The reduced coupling could inhibit the photocycle in several ways: (i) by greatly reducing the equilibrium concentration of the all-trans form of the retinal that is capable of isomerization and storing the energy upon light absorption; (ii) by changing the structure of the active site so that upon photoisomerization, the system changes to another state of equal free energy with no net energy storage; or (iii) by photoisomerization of the system with even the formation of a K- and L-type intermediate (as seen in blue pmbR) (55), but the reaction path during the cycle is changed such that the final reduction of the pK_a of PSB (required for its deprotonation) would not occur (29, 32, 38, 40, 55).

The blue-to-purple transition might or might not involve a change in the conformation of the entire protein molecule, as we only see a very small portion of it—i.e., the active site. In any case, the transition will occur at a pH when the free energies of the blue (b) and purple (p) conformations are equal—thus, for $bR_b = bR_p$, $\Delta G = 0 = \Delta H - T\Delta S$. ΔH depends on the interaction energy between the surface potential and the different internal charges and dipoles of the protein residues as well as the electrostatic interaction between the charges and dipoles of the protein residues (38, 40, 54). ΔS depends on the ionic charges and the water organization on the surface as well as the structure within the protein in the two conformations. A large change in both the entropy and enthalpy terms would be predicted if pH changes alter the acid–base equilibrium of the different acid groups of the protein and/or the lipids.

In conclusion, the pH at which the blue-to-purple transition occurs should depend on the surface potential (i.e., the pH and ionic strength of the medium as well as the type of lipid or micelles used in reconstituting bR) and the internal protein structure that controls conformation of the active site. The conformations of the blue or the purple forms will probably differ in different species (pmbR, ebR, and Y185F). The only common factor is that the blue forms have weak coupling to their counterions (thus their absorption is shifted to the lower energies and do not lead to proton pumping). The purple forms have higher absorption energies resulting from stronger coupling to the counterions and can therefore store

energy upon photoisomerization, which leads to the proper conformation changes required for the deprotonation of the PSB (29) and, thus, to proton pumping.

M.A.E. wishes to thank Dr. A. Warshel for useful discussions. The work at the University of California at Los Angeles was supported by the Department of Energy, Office of Basic Energy Sciences (Grant DE-FG03-88ER13828). The work at the Massachusetts Institute of Technology was supported by National Institutes of Health Grant GM28289-09 and an Office of Naval Research Grant N00014-82-K-0668.

1. Oesterhelt, D. & Stoeckenius, W. (1971) *Nature (London) New Biol.* **233**, 149–152.
2. Stoeckenius, W. & Bogomolni, R. A. (1982) *Annu. Rev. Biochem.* **52**, 587–619.
3. Bridgen, J. & Walker, I. D. (1976) *Biochemistry* **15**, 792–798.
4. Bayley, H., Huang, K. S., Radhakrishnan, R., Ross, A. H., Takagaki, Y. & Khorana, H. G. (1981) *Proc. Natl. Acad. Sci. USA* **78**, 2225–2229.
5. Lozier, R., Bogomolni, R. A. & Stoeckenius, W. (1975) *Biophys. J.* **15**, 215–278.
6. Mathies, R. A., Cruz, C. H., Pollard, W. T. & Shank, C. V. (1988) *Science* **240**, 777–779.
7. Dencher, N. & Wilms, M. (1975) *Biophys. Struct. Mech.* **1**, 259–271.
8. Stoeckenius, W. (1979) *Biochem. Biophys. Acta* **505**, 215–279.
9. Lo, K.-M., Jones, S. S., Hackett, N. R. & Khorana, H. G. (1984) *Proc. Natl. Acad. Sci. USA* **81**, 2285–2289.
10. Gilles-Gonzalez, M. A., Hackett, N. R., Jones, S. J., Khorana, H. G., Lee, D.-S., Lo, K.-M. & McCoy, J. M. (1986) *Methods Enzymol.* **125**, 190–214.
11. Khorana, H. G. (1988) *J. Biol. Chem.* **263**, 7439–7442.
12. Nassal, M., Mogi, T., Karnik, S. S. & Khorana, H. G. (1987) *J. Biol. Chem.* **262**, 9264–9270.
13. Braiman, M. S., Mogi, T., Stern, L. J., Hackett, N. R., Chao, B. H., Khorana, H. G. & Rothschild, K. J. (1988) *Proteins: Struct. Funct. Genet.* **3**, 219–229.
14. Dunn, R. J., Hackett, N. R., McCoy, J. M., Chao, B. H., Kimura, K. & Khorana, H. G. (1987) *J. Biol. Chem.* **262**, 9246–9254.
15. Karnik, S. S., Nassal, M., Doi, T., Jay, E., Sgaramella, V. & Khorana, H. G. (1987) *J. Biol. Chem.* **262**, 9255–9263.
16. Braiman, M. S., Stern, L. J., Chao, B. H. & Khorana, H. G. (1987) *J. Biol. Chem.* **262**, 9271–9276.
17. Mogi, T., Stern, L. J., Hackett, N. R. & Khorana, H. G. (1987) *Proc. Natl. Acad. Sci. USA* **84**, 5595–5599.
18. Mogi, T., Stern, L. J., Marti, T., Chao, B. H. & Khorana, H. G. (1988) *Proc. Natl. Acad. Sci. USA* **85**, 4148–4152.
19. Holz, M., Drachev, L. A., Mogi, T., Otto, H., Kaulen, A. D., Heyn, M. P., Skulachev, V. P. & Khorana, H. G. (1989) *Proc. Natl. Acad. Sci. USA* **86**, 2167–2171.
20. Stern, L. J., Hackett, N. R., Braiman, M. S., Chao, B. H. & Khorana, H. G. (1987) *Biophys. J.* **51**, 145a (abstr.).
21. Ahl, P. L., Hackett, N. R., Rothschild, K. J. & Khorana, H. G. (1987) *Biophys. J.* **51**, 146a (abstr.).
22. Ahl, P. L., Stern, L. J., Durig, D., Mogi, T., Khorana, H. G. & Rothschild, K. J. (1988) *J. Biol. Chem.* **263**, 13594–13601.
23. Nagle, J. F. & Morowitz, H. J. (1978) *Proc. Natl. Acad. Sci. USA* **75**, 298–302.
24. Stoeckenius, W. (1979) *Membrane Transduction Mechanisms*, eds. Come, R. A. & Dowling, J. E. (Raven, New York), pp. 39–47.
25. Merz, H. & Zundel, G. (1981) *Biochem. Biophys. Res. Commun.* **101**, 540–546.
26. Bogomolni, R. A., Stubbs, L. & Lanyi, J. (1978) *Biochemistry* **17**, 1037–1041.
27. Hess, B. & Kuschmitz, D. (1979) *FEBS Lett.* **100**, 334–340.
28. Kalisky, O., Ottolenghi, M., Honig, B. & Korenstein, R. (1981) *Biochemistry* **20**, 649–655.
29. Hanamoto, J. H., Dupuis, P. & El-Sayed, M. A. (1984) *Proc. Natl. Acad. Sci. USA* **81**, 7083–7087.
30. Khorana, H. G., Gerber, G. E., Herlihy, W. C., Gray, C. P., Anderegg, R. J., Nihei, K. & Beimann, K. (1979) *Proc. Natl. Acad. Sci. USA* **76**, 5046–5050.
31. Rothschild, K. J., Roepe, P., Ahl, P. L., Earnest, T. N., Bogomolni, R. A., Das Gupta, S. K., Mulliken, C. M. & Herzfeld, J. (1986) *Proc. Natl. Acad. Sci. USA* **83**, 347–351.
32. Chronister, E. L. & El-Sayed, M. A. (1987) *Photochem. Photobiol.* **45**, 507–513.
33. Moore, T. A., Edgerton, M. E., Parr, G., Greenwood, C. & Perham, R. N. (1978) *Biochem. J.* **171**, 469–476.
34. Mowery, P. C., Lozier, R. H., Chae, Q., Tseng, Y.-W., Taylor, M. & Stoeckenius, W. (1979) *Biochemistry* **18**, 4100–4107.
35. Muccio, D. D. & Cassim, J. Y. (1979) *J. Mol. Biol.* **135**, 595–609.
36. Kimura, Y., Ikegami, A. & Stoeckenius, W. (1984) *Photochem. Photobiol.* **40**, 641–650.
37. Fischer, U. & Oesterhelt, D. (1979) *Biophys. J.* **28**, 211–230.
38. Corcoran, T. C., Ismail, K. Z. & El-Sayed, M. A. (1987) *Proc. Natl. Acad. Sci. USA* **84**, 4094–4098.
39. Jang, D.-J., Corcoran, T. C. & El-Sayed, M. A. (1988) *Photochem. Photobiol.* **48**, 209–217.
40. Jang, D.-J. & El-Sayed, M. A. (1988) *Proc. Natl. Acad. Sci. USA* **85**, 5918–5922.
41. Szundi, I. & Stoeckenius, W. (1987) *Proc. Natl. Acad. Sci. USA* **84**, 3681–3684.
42. Szundi, I. & Stoeckenius, W. (1988) *Biophys. J.* **54**, 227–232.
43. Szundi, I. & Stoeckenius, W. (1989) *Biophys. J.* **56**, 369–383.
44. Jang, D.-J., El-Sayed, M. A., Mogi, T., Stern, L. J. & Khorana, H. G. (1990) *FEBS Lett.*, in press.
45. Lind, C., Hojeberg, B. & Khorana, H. G. (1981) *J. Biol. Chem.* **256**, 8298–8305.
46. Hackett, N. R., Stern, L. J., Chao, B. H., Kronis, K. A. & Khorana, H. G. (1987) *J. Biol. Chem.* **262**, 9277–9284.
47. Popot, J.-L., Gerchamn, S.-E. & Engelman, D. M. (1987) *J. Mol. Biol.* **198**, 655–676.
48. Herzfeld, J., Das Gupta, S. K., Farrar, M. R., Harbison, G. S., McDermott, A. E., Pelletier, S. L., Raleigh, D. P., Smith, S. O., Winkel, C., Lugtenburg, J. & Griffin, R. G. (1990) *Biochemistry*, in press.
49. Maeda, A., Ogura, T. & Kitagawa, T. (1986) *Biochemistry* **25**, 2798–2803.
50. Bogomolni, R. A., Stubbs, L. & Lanyi, T. K. (1978) *Biochemistry* **17**, 1037–1041.
51. Fukumoto, J. M., Hopewell, W. D., Karvaly, B. & El-Sayed, M. A. (1981) *Proc. Natl. Acad. Sci. USA* **78**, 252–255.
52. Jang, D.-J. & El-Sayed, M. A. (1989) *Proc. Natl. Acad. Sci. USA* **86**, 5815–5819.
53. Chronister, E. L., Corcoran, T. C., Song, L. & El-Sayed, M. A. (1986) *Proc. Natl. Acad. Sci. USA* **83**, 8530–8584.
54. Warshel, A. & Russell, S. T. (1984) *Q. Rev. Biophys.* **17**, 283–422.
55. El-Sayed, M. A. (1988) *Int. J. Quantum Chem. Quantum Chem. Symp.* **22**, 367–375.